A comparison between linear and exponential schemes in control volume finite element method

H. Abbassi
Faculté des Sciences, Département de Physique, Tunisia
A. Boughamoura and S. Ben Nasrallah
Ecole Nationale d'Ingénieurs de Monastir, Laboratoire d'Etudes des Systèmes Thermiques et Energétiques, Monastir, Tunisia

Received November 2001
Revised January 2003
Accepted January 2003

Keywords *Finite element method, Fluid flow, Incompressible flow*

Abstract *In this paper, we present a comparison of linear and exponential interpolation functions for control volume finite element method. The exponential interpolation function is expressed in the elemental local coordinate system whereas the classic linear interpolation function is expressed in the global coordinate system. The comparison is achieved in the case of the Green-Taylor vortex, a flow from which we know the analytical solution. Firstly, the two functions are applied to a triangular element of the domain to compare the results given by each interpolation function to the exact value. Secondly, these two functions are compared when used to solve the discretized equations over the entire domain.*

Nomenclature

$\mathbf{J}_i$ = combined convection diffusion flux corresponding to the component u_i
L = elemental side
$\mathbf{n}$ = outward-pointing normal
P = node
p = pressure
Pe_Δ = elemental Peclet number
Re = Reynolds number
s_i = body force
S = surface bounding the control volume
$\mathbf{u}$ = velocity vector
$\mathbf{u}_{\mathrm{av}}$ = average velocity vector over an element
U_{av} = magnitude of vector $\mathbf{u}_{\mathrm{av}}$
u_i = velocity components ($u_1 = u$, $u_2 = v$)
$\tilde{u}, \tilde{v}$ = pseudo-velocity components
V_p = control volume
x, y = global Cartesian coordinates
X, Y = local Cartesian coordinates

Greek symbols

μ = dynamic viscosity of the fluid
ρ = density of the fluid
τ = dimensionless time
$\Delta\tau$ = dimensionless time step

Subscripts

av = average
i = ith Cartesian direction
nb = neighboring nodes to the central node
P = pertaining to node P

Abbreviations

CVFEM = control volume finite element method
FLO = flow-oriented interpolation
FLOS = flow-oriented interpolation with source effects
LI = linear interpolation
LU = lower-upper

International Journal of Numerical Methods for Heat & Fluid Flow
Vol. 13 No. 4, 2003
pp. 403-414

0961-5539
DOI 10.1108/09615530310475885

1. Introduction

The numerical procedure used in this study is the control volume finite element method (CVFEM) in equal order; i.e. pressure and velocity components are stored at the same point. CVFEM combines advantages of finite element and finite volume methods. Its formulation is based on easy physical interpretation and their solutions satisfy both global and local conservation. In addition, CVFEM uses a control volume that is not obligatory regular and then can delimit a complicate domain. The flexibility of the grid is the famous advantage of this method. Baliga and Patankar (1980, 1983) were the first founders of the CVFEM. Besides the introduction of the basic concept of using the control volume, the major contribution of their work lies in the development of an appropriate shape function for simulating a convection diffusion process. Over each element, the proposed shape function is exponential in the direction of the average velocity vector and linear in the normal direction. This function called flow-oriented interpolation (FLO) simulates correctly the one-sided (upwind) nature of convection and the two-sided nature of diffusion. Baliga and Patankar (1980) mentioned that, since FLO is developed along the direction of the local flow, it reduces crosswind diffusion considerably. Since that time, many transformations have been carried to FLO. Prakash (1986) proposed an other shape function similar to FLO but depending on the source terms of the momentum equations. This function is called flow-oriented interpolation with sources effects (FLOS). He used FLOS also in the integration of the continuity equation for formulating the pressure equation. Under certain conditions FLOS is an exact solution of the equation of two-dimensional convection-diffusion problem written in the local coordinate system. FLOS proposed by Prakash (1986) is not the unique solution of the above-mentioned equation. In this context, Hookey (1989) proposed an other variant of FLOS which differently depends on the source term. Saabas and Baliga (1994) carried out a detailed investigation about interpolation functions used in CVFEM for two- and three-dimensional incompressible fluid flow. Their study concerns FLO, FLOS and mass-weighted (MAW) upwind scheme. They conclude that the FLOS scheme is not recommended, it is even more prone to difficulties than the FLO scheme. Even in source dominated problems for which both the FLO and FLOS scheme produce converged solutions, the results of the FLOS scheme are not necessarily more accurate than those produced by the FLO scheme. Furthermore, to the study of Saabas and Baliga (1994), FLOS and FLO are completely abandoned in the treatment of the continuity equation and in the diffusive term of momentum equations and were replaced by a simple linear interpolation (LI) expressed in the global coordinate system. FLO is retained only in the treatment of the convective term of the momentum equations. Then, it seems that the golden time of the exponential interpolation is coming to its finish.

The principle aim of this paper is the evaluation of FLO as it was developed by Saabas and Baliga (1994) by comparing it to the classic LI. LI and FLO

schemes are the most used in CVFEM. We will try to answer a question that we judge very important: Does the FLO used in the convective term present any advantage compared to LI? In order to have a precise comparison, we have chosen to apply FLO and LI to a flow from we know which is the exact solution. Unfortunately, flows verifying this condition are very few. The flow between concentric rotating cylinders have exact solutions that do not depend on the Reynolds number Re, variation of errors cannot be calculated as a function of Re. Also, we have not chosen the Pearson test of Pearson (1965) because solutions are obtained only for a Re equal to unity. Finally, we retain the Green-Taylor vortex flow. In this example, exact solutions depend on the Re and on the time. This flow constitutes a good example for the evaluation of the precision of FLO and LI.

2. Governing equations – numerical procedure

The mass conservation and the Navier-Stokes equations for incompressible Newtonian fluid flow are given as follows:

$$\nabla \cdot (\rho \mathbf{u}) = 0 \tag{1}$$

$$\frac{\partial u_i}{\partial \tau} + \nabla \cdot (\mathbf{J}_i) = s_i - \frac{\partial p}{\partial x_i} \tag{2}$$

where

$$\mathbf{J}_i = \rho \mathbf{u} u_i - \mu \nabla u_i \tag{3}$$

In these equations, μ is the dynamic viscosity, ρ is the mass density and p is the pressure. s_i is the body force term acting in the ith Cartesian coordinate direction and $\mathbf{J}_i$ is the combined convection-diffusion flux associated to the component u_i of the velocity vector $\mathbf{u}$. Since we are limited to two-dimensional problems i can take only two values: for $i = 1 : u_i = u, x_i = x$ and for $i = 2 : u_i = v, x_i = y$.

We now present a brief description of the discretization procedure in CVFEM used in equal order. Detail descriptions of this method for fluid flow are available in all references cited earlier, except Pearson (1965), in the two publications of Abbassi *et al.* (2001a, b) and in many other references. A control volume is constructed around every node P by joining the centroids of the relevant triangles to the midpoints of the sides as indicated in Figure 1.

The momentum transport equation (2) are integrated over the control volume to obtain equations of nodal values of the velocity components. A special procedure is used to integrate the mass conservation equation (1) leading to the discretized pressure equation. Using the Green-Ostrograski theorem, integration of the divergence term in momentum equation (2) over the control volume surrounding node P gives:

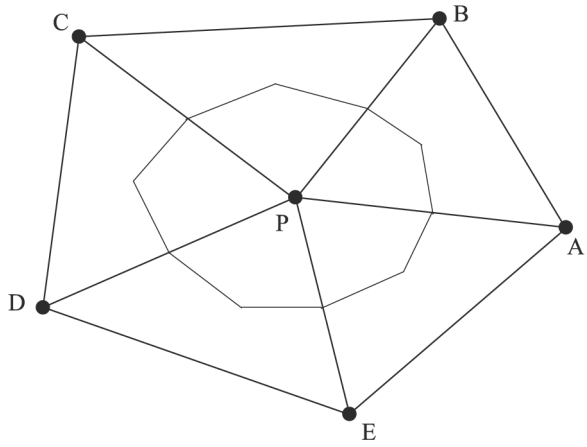

Figure 1.
Control volume around a node P

$$\int_{V_p} \nabla \cdot (\mathbf{J}_i)\, \mathrm{d}v = \int_S \mathbf{J}_i \cdot \mathbf{n}\, \mathrm{d}s \tag{4}$$

where S is the surface area of the control volume V_p surrounding node P and $\mathbf{n}$ is a unit outward normal to the differential surface area ds.

Now we consider the element PAB shown in Figure 2 associated to a local FLO Cartesian coordinate system (X, Y), the origin is located at the element centroid g and the X-axis is aligned with the elemental-averaged velocity vector as indicated in Figure 2. This local coordinate system is used by the FLO scheme. The second member of equation (4) is evaluated by calculating the flux of $\mathbf{J}_i$ throughout the surface bounding the control volume situated in every element neighboring node P. Integration of other terms in equation (2) over the control volume can be realized easily. By collecting and simplifying, the discretized equations for u and v components can be written as:

$$A_{\mathrm{P}} u_p = \sum_{\mathrm{nb}} A_{\mathrm{nb}} u_{\mathrm{nb}} + V_p \left\langle -\frac{\partial p}{\partial x} \right\rangle + V_p u_p^{\mathrm{o}} / \Delta\tau \tag{5}$$

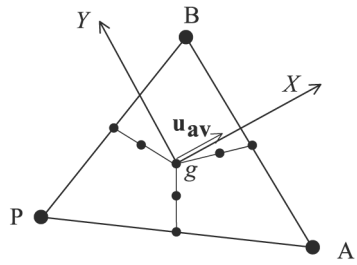

Figure 2.
Element PAB with local coordinate system and seven internal nodes. These seven internal nodes will be used later

$$A_P v_p = \sum_{nb} A_{nb} v_{nb} + V_p \left\langle -\frac{\partial p}{\partial y} \right\rangle - V_p v_p^o / \Delta\tau \tag{6}$$

where subscript nb refers to all nodes neighboring to the node P, $\Delta\tau$ is the time step, u_p^o and v_p^o refers to the last time step values of u_p and v_p. $\left\langle -\frac{\partial p}{\partial x} \right\rangle$ and $\left\langle -\frac{\partial p}{\partial y} \right\rangle$ are the average values of $\left(-\frac{\partial p}{\partial x}\right)$ and $\left(-\frac{\partial p}{\partial y}\right)$ acting over the entire control volume surrounding the node P and is evaluated by assuming a linear variation of pressure.

The pressure equation is indirectly specified through satisfaction of mass conservation equation (1). Equations (5) and (6) can be rewritten as:

$$u_p = \tilde{u}_p + B_p \left\langle -\frac{\partial p}{\partial x} \right\rangle \tag{7}$$

$$v_p = \tilde{v}_p + B_p \left\langle -\frac{\partial p}{\partial y} \right\rangle \tag{8}$$

where $\tilde{u}_p$ and $\tilde{v}_p$ represents the pseudo-velocity components, and B_p the pressure-gradient coefficient. Their expressions are easily identified by comparing equations (7) and (8), respectively, to equations (5) and (6).

As in Saabas and Baliga (1994), we assume a linear variation of u and v components in the treatment of the pressure equation. Using equations (7) and (8), the integration of the mass conservation equation (1) through the control volume surrounding node P yields the discretized equation of pressure written in the classic form:

$$C_p P_p = \sum_{nb} C_{nb} P_{nb} + D_p \tag{9}$$

where D_p is the source term arising from pseudo-velocity fields.

The SIMPLER algorithm of Patankar (1980) was applied to treat the pressure-velocity coupling. Equations (5), (6) and (9) are written in a matrix shape and solved iteratively at every instant by LU decomposition.

3. Interpolation functions

The interpolation functions that will be discussed here are for the velocity components u_i, when they are treated as transported scalars in the appropriate momentum equations. The vector $\mathbf{J}_i$ in equation (2) contains a convective term ($\rho \mathbf{u} u_i$) and a diffusive term ($\mu \nabla u_i$). In this investigation, interpolation functions concern only the u_i component in the convective term. The work of Saabas and Baliga (1994) show that the adequate interpolation function for u_i in the diffusive term and in the treatment of the continuity equation is the LI scheme. The simplest interpolation function, that first comes to the mind, is the LI which is usually expressed in the global coordinate system by:

$$u_i = ax + by + c \tag{10}$$

Writing equation (10) at the three nodes of a triangular element, where u_i is given, we can easily deduce values of the coefficients a, b and c. Consider now the triangular element PAB shown in Figure 2, the relation between the local and the global coordinate system is given by:

$$X = \frac{1}{U_{\text{av}}}[(x - x_g)u_g + (y - y_g)v_g] \tag{11}$$

$$Y = \frac{1}{U_{\text{av}}}[-(x - x_g)v_g + (y - y_g)u_g] \tag{12}$$

where the subscript g refers to the elemental centroid and U_{av} is the magnitude of the average velocity vector $\mathbf{u}_{\text{av}}$ of the triangular element. The exponential interpolation function concerned in this study, called FLO is proposed by Saabas and Baliga (1994):

$$u_i = A\xi + BY + C \tag{13}$$

the variable ξ is defined as:

$$\xi = \frac{\mu}{\rho U_{\text{av}}}\left\{-1 + \exp\frac{\text{Pe}_\Delta(X - X_{\max})}{X_{\max} - X_{\min}}\right\}$$

the elemental Peclet number (Pe_Δ) is an indicator of the relative strengths of convection to diffusion within the element and defined as:

$$\text{Pe}_\Delta = \frac{\rho U_{\text{av}}(X_{\max} - X_{\min})}{\mu}$$

with $X_{\max}$ and $X_{\min}$ defined as:

$$X_{\max} = \text{MAX}(X_{\text{P}}, X_A, X_B) \text{ and } X_{\min} = \text{MIN}(X_{\text{P}}, X_A, X_B)$$

4. Green-Taylor vortex

Exact solutions of the Green-Taylor vortex are given as:

$$u = -\cos(x)\sin(y)\exp(-2\tau/\text{Re}) \tag{14}$$

$$v = \sin(x)\cos(y)\exp(-2\tau/\text{Re}) \tag{15}$$

$$p = -\frac{1}{4}[\cos(2x) + \cos(2y)]\exp(-4\tau/\mathrm{Re}) \tag{16}$$

The numerical domain considered in this study is a square of side π in which x and y are in the range of $-\pi/2$ and $\pi/2$. Figure 3 is a plot of the velocity field of the Green-Taylor vortex at $\tau = 1$ and $\mathrm{Re} = 100$ computed using the LI scheme.

5. Application over an element

The triangular element PAB in which we will compare the FLO and the LI schemes is indicated in Figure 2. Values of u_i at nodes P, A and B are given and serve to calculate the coefficients of the interpolation functions (10) and (13). Calculated values of u_i at the seven internal nodes are deduced using either FLO (13) or LI (10). Since most software of triangularisation have tendency to construct equilateral elements, the element of Figure 2 is also equilateral and of a side L. It should be noted that values of u_i at the seven internal nodes are used to obtain the discretized equations of the entire domain in CVFEM.

We define the local error in percent committed in the calculation of u_i at a given internal node as:

$$\mathrm{e}(I) = \left|\frac{u_i(\text{exact}) - u_i(\text{calculated})}{u_i(\text{exact})}\right| \times 100 \tag{17}$$

where $I = 1,\ldots,7$ represents the issue of the internal node, u_1 and u_2 are, respectively, u and v components.

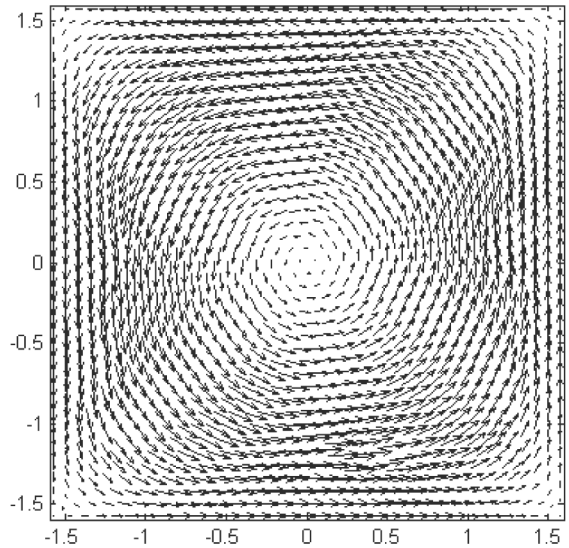

Figure 3.

The global error relative to the triangular element is defined as:

$$\text{error}(u_i) = \max[\text{e}(I)] \tag{18}$$

The triangular element PAB is placed in the calculation domain so that the node P is placed at the point of coordinates $(x = 1, y = 1)$. We note that error(u) and error(v) are found to be almost in the same magnitude, so, only error(u) will be presented in this section.

Figure 4 is a plot of the variation of error(u) as a function of the elemental side L. Starting from a very small value of L, curves corresponding to FLO and LI overlap. This result is expected, as if L tends to zero, Pe_Δ also tends to zero and the FLO scheme given by equation (13) is identical to the LI scheme given by equation (10). By increasing the side L, the error given by the FLO becomes more pronounced compared to that given by the LI scheme. Figure 4 shows clearly that over an element the LI scheme is far more accurate than the FLO scheme. This result is confirmed in Figure 5 where we plot the variation of error(u) as a function of Pe_Δ.

Pe_Δ is varied by varying the global Re and keeping fixed the value of L at 0.01. The relation between Pe_Δ and Re is given by:

$$\text{Pe}_\Delta = U_{\text{av}}\,(X_{\max} - X_{\min})\,\text{Re} \tag{19}$$

As seen in Figure 5, the LI scheme is clearly more accurate than the FLO scheme.

6. Application over the entire domain

The discretized equations (5), (6) and (9) are solved using the SIMPLER algorithm for the Green-Taylor vortex over the entire domain which is a square

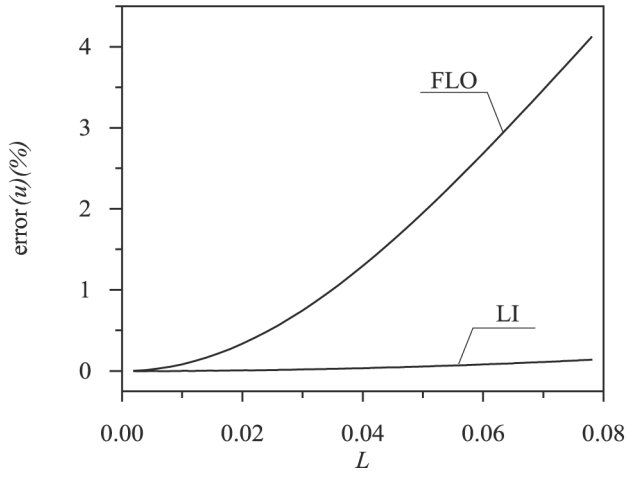

Figure 4.
Variation of error(u) as a function of the elemental side L

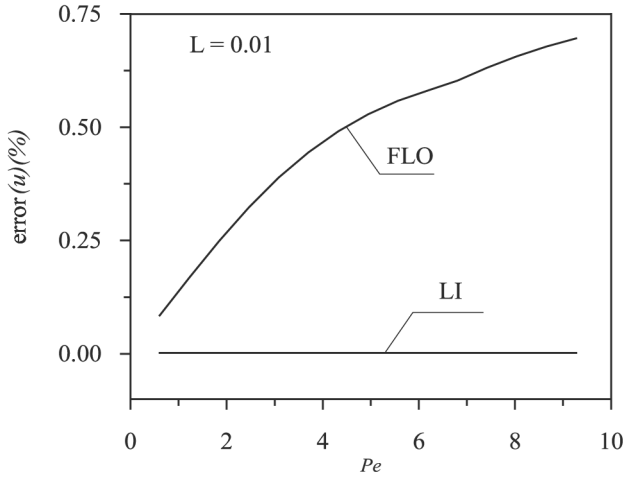

Figure 5.
Variation of error (u) as a function of the Pe_{Δ}

of side π as shown in Figure 3. Computed solutions are compared to the exact solutions given by equations (14)-(16). The overall error is defined as:

$$\text{error}(\phi)\frac{\sum|\phi\,(\text{exact}) - \phi\,(\text{calculated})|}{\sum|\phi\,(\text{exact})|} \times 100 \tag{20}$$

where the summation is taken over all nodes of the calculation domain and ϕ is the dependent variable ($\phi = u, v, p$). Here also error(u) and error(v) are found to be almost of the same magnitude, so in the following, only error(u) and error(p) will be presented. error(p) is calculated not to test the interpolation function of pressure but to evaluate the effects of LI and FLO on the evolution of pressure field. Results are obtained by a grid of 3,369 nodes and 6,524 elements. This grid shown in Figure 6 is slightly more refined than the most refined grid used by Braza (1981) with a classic control volume method (3,136 nodes). A more refined grid of 4,739 nodes and 9,224 elements does not carry any significant change on the numerical results.

The purpose of this paragraph is the comparison of the effects of FLO and LI schemes on the stability of the numerical process and on the accuracy of solutions. Starting from exact fields of u and v obtained by equations (14) and (15) for $\tau = 0$ and Re = 100 and from an identical zero field for pressure, the numerical process is abandoned to itself and stopped at $\tau = 1$. During the numerical process, boundary conditions for u and v components are fixed at their values given by equations (14) and (15) at $\tau = 1$ and Re = 100. Pseudo-velocity components $\tilde{u}$ and $\tilde{v}$ are equal to u and v components, respectively, at all boundaries.

The distance of fluid travel in one time increment must be less than one space increment (Δx or Δy). This hypothesis leads to the constraint on the time step $\Delta\tau$ given as:

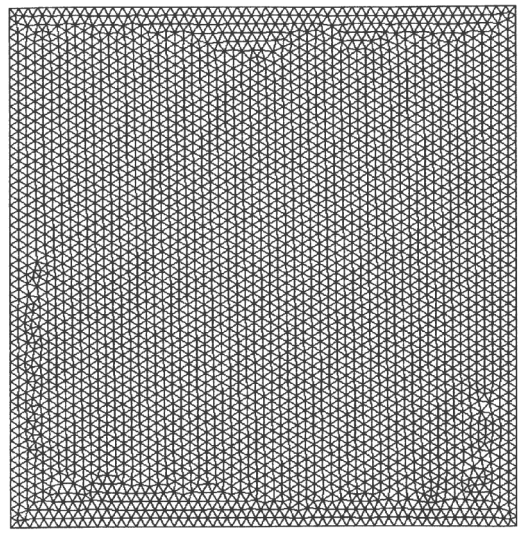

Figure 6.

$$\Delta\tau < \left\{ \min\left(\frac{\Delta x}{|u|}, \frac{\Delta y}{|v|} \right) \right\} \tag{21}$$

In this study, $\Delta x = \Delta y = 0.06$ and the maximum values of u or v is equal to 1. The constraint (21) allows to $\Delta\tau < 0.06$. In the following, the time step is fixed at $\Delta\tau = 0.05$. A value of $\Delta\tau = 0.025$ was also tested but no significant change was observed on the numerical results.

As can be seen in Figure 7, where we plot the evolution of error(u) as a function of time, the curve corresponding to the LI scheme leads to damping oscillations, while error(u) corresponding to the FLO scheme increases considerably and it seems that the numerical process will diverge if the time is sufficiently prolonged. As given by equations (14) and (15), u and v components are strongly decreasing functions of time. As the time is prolonged, values of u and v becomes small and then the elemental average velocity U_{av} is also small and may tend to zero in some nodes. Local coordinate system (X, Y) calculated by equations (11) and (12) and the function ξ of equation (13) may lead to unrealistic values. This may explain why the FLO scheme seems to diverge. This is a real handicap; the FLO scheme can not predict correctly a flow or a region of flow when velocities are small. Especially, FLO should not be used in flows containing rolls such as shedding vortices behind obstacle and convective cells due to heat transfer.

Figure 8 compares error(p) obtained by FLO to that obtained by LI. We remark that both schemes lead to damping oscillations but oscillations of the LI are of less magnitude. The variation of error($\phi = u, v, p$) as a function of the Re has been also realized. Results show that for Re ranging from 10 to 500, the LI

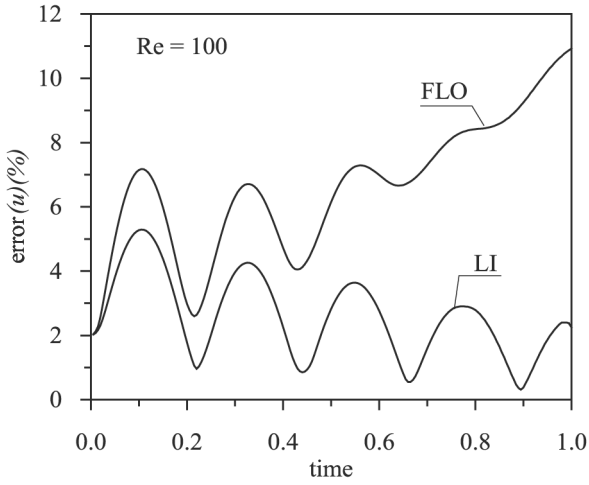

Figure 7.
Evolution of error(u)

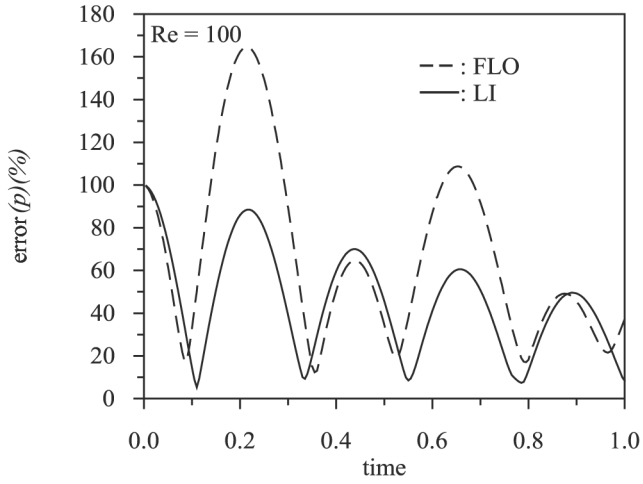

Figure 8.
Evolution of error(p)

scheme leads always to more accurate solutions than those given by the FLO scheme. Beyond Re $\cong$ 500 oscillations, growth in magnitude for LI and FLO and the number of iterations per time step augments considerably and the convergence of the numerical process becomes difficult to realize.

Patankar (1980) showed that the centered scheme for classic volume, which is equivalent to LI scheme in CVFEM, is tolerated only for low Re. The principle cause is that the centered scheme produces "numerical diffusion". This cause is realistic because the control volume used in two-dimensional classic control volumes is rectangular and then has only four faces, then

numerical diffusion can easily happen. Other interpolation functions are then proposed such as upwind and exponential schemes. In CVFEM the grid is not structured, the control volume has far more faces than that in classic volume. In CVFEM a given node has in general five to eight neighboring nodes, thus the control volume around this node has 10-16 faces. In this configuration, we estimate that the numerical diffusion produced by the LI scheme has secondary effects on the accuracy of the numerical results. This may explain the superiority of the LI scheme on the FLO scheme in CVFEM.

7. Conclusion

The linear interpolation and the exponential interpolation schemes used in CVFEM are compared in the case of the Green-Taylor vortex, a flow from which we know the analytical solutions. Results show that, over a triangular element, the linear interpolation gives solutions more accurate than those given by the exponential scheme. Over the calculation domain, the resolution of the system of discretized equations show that the linear function leads to less oscillations and more accurate solutions than the exponential function in spite of its complications.

References

Abbassi, H., Turki, S. and Ben Nasrallah, S. (2001a), "Mixed convection in a plane channel with a built-in triangular prism", *Numerical Heat Transfer, Part A*, Vol. 39 No. 3, pp. 307-20.

Abbassi, H., Turki, S. and Ben Nasrallah, S. (2001b), "Numerical investigation of forced convection in a plane channel with a built-in triangular prism", *Int. J. Therm. Sci.*, Vol. 40, pp. 649-58.

Baliga, B.R. and Patankar, S.V. (1980), "A new finite element formulation for convection-diffusion problems", *Numerical Heat transfer*, Vol. 3, pp. 393-410.

Baliga, B.R. and Patankar, S.V. (1983), "A control volume finite element method for two dimensional fluid flow and heat transfer", *Numerical Heat transfer*, Vol. 6, pp. 245-62.

Braza, M. (1981), "Simulation numérique du décollement instationnaire externe par une formulation vitesse-pression", Application à l'écoulement autour d'un cylindre, Thèse, Institut National Polytechnique de Toulouse.

Hookey, N.A. (1981), "A CVFEM for two-dimensional viscous compressible fluid flow", PhD thesis, Department of Mechanical Engineering, McGill University, Montreal, Que.

Patankar, S.V. (1980), "Numerical heat transfer and fluid flow", *Series in Comp. Meth. in Mech. and Therm. Sc.*, McGraw-Hill, NY, USA.

Pearson, C.E. (1965), "A computational method for viscous flow problems", *J. Fluid Mech.*, Vol. 21, pp. 611-22.

Prakash, C. (1986), "An improved control volume finite-element method for heat and mass transfer, and for fluid flow using equal-order velocity-pressure interpolation", *Numerical Heat transfer*, Vol. 9, pp. 253-76.

Saabas, H.J. and Baliga, B.R. (1994), "Co-located equal-order control-volume finite-element method for multidimensional, incompressible, fluid flow part I: formulation", *Numerical Heat Transfer, Part B*, Vol. 26, pp. 381-407.